Title: The PARP inhibitor PJ-34 sensitizes cells to UVA-induced phototoxicity by a PARP independent mechanism

Author: Petra Lakatos Csaba Hegedűs Nerea Salazar Ayestarán Ángeles Juarranz Katalin E. Kövér Éva Szabó László Virág

PII: S0027-5107(16)30115-4
DOI: http://dx.doi.org/doi:10.1016/j.mrfmmm.2016.07.001
Reference: MUT 11559

To appear in: *Mutation Research*

Received date: 16-2-2016
Revised date: 28-5-2016
Accepted date: 4-7-2016

Please cite this article as: Petra Lakatos, Csaba Hegedűs, Nerea Salazar Ayestarán, Ángeles Juarranz, Katalin E.Kövér, Éva Szabó, László Virág, The PARP inhibitor PJ-34 sensitizes cells to UVA-induced phototoxicity by a PARP independent mechanism, Mutation Research/Fundamental and Molecular Mechanisms of Mutagenesis http://dx.doi.org/10.1016/j.mrfmmm.2016.07.001

The PARP inhibitor PJ-34 sensitizes cells to UVA-induced phototoxicity by a PARP independent mechanism

Petra Lakatos[1], Csaba Hegedűs[1] Nerea Salazar Ayestarán[2], Ángeles Juarranz[2], Katalin E. Kövér[3], Éva Szabó[4] and László Virág[1,5,#],

[1]Department of Medical Chemistry, Faculty of Medicine, University of Debrecen, Debrecen, Hungary

[2]Department of Biology, Faculty of Sciences, Universidad Autónoma of Madrid, 28049-Madrid, Spain

[3]Department of Inorganic and Analytical Chemistry, Faculty of Sciences, University of Debrecen, Debrecen, Hungary

[4]Department of Dermatology, Faculty of Medicine, University of Debrecen, Debrecen, Hungary

[5]MTA-DE Cell Biology and Signaling Research Group, Debrecen, Hungary

[#]Correspondence should be addressed to:

László Virág M.D., D.Sc.

Department of Medical Chemistry

Faculty of Medicine, University of Debrecen

Nagyerdei krt 98. H-4032 Debrecen, Hungary

e-mail: lvirag@med.unideb.hu

Tel: +36-52-412-345

Highlights

PARP-1 is not a key regulator of photochemotherapy.
The PARP inhibitor PJ-34 sensitizes cells to UVA-induced phototoxicity by a PARP independent mechanism.
Photosensitization by PJ-34 is associated with increased ROS production and DNA damage.
Cells sensitized by PJ-34 undergo caspase-mediated apoptosis.

Abstract

A combination of a photosensitizer with light of matching wavelength is a common treatment modality in various diseases including psoriasis, atopic dermatitis and tumors. DNA damage and production of reactive oxygen intermediates may impact pathological cellular functions and viability. Here we set out to investigate the role of the nuclear DNA nick sensor enzyme poly(ADP-ribose) polymerase 1 in photochemical treatment (PCT)-induced tumor cell killing. We found that silencing PARP-1 or inhibition of its enzymatic activity with Veliparib had no significant effect on the viability of A431 cells exposed to 8-methoxypsoralen (8-MOP) and UVA (2.5 J/cm^2) indicating that PARP-1 is not likely to be a key player in either cell survival or cell death of PCT-exposed cells. Interestingly, however, another commonly used PARP inhibitor PJ-34 proved to be a photosensitizer with potency equal to 8-MOP. Irradiation of PJ-34 with UVA caused changes both in the UV absorption and in the 1H NMR spectra of the compound with the latter suggesting UVA-induced formation of tautomeric forms of the compound. Characterization of the photosensitizing effect revealed that PJ-34+UVA triggers overproduction of reactive oxygen species, induces DNA damage, activation of caspase 3 and caspase 8 and internucleosomal DNA fragmentation. Cell death in this model could not be prevented by antioxidants (ascorbic acid, trolox, glutathione, gallotannin or cell permeable superoxide dismutase or catalase) but could be suppressed by inhibitors of caspase-3 and -8. In conclusion, PJ-34 is a photosensitizer and PJ-34+UVA causes DNA damage and caspase-mediated cell death independently of PARP-1 inhibition.

Keywords: ultraviolet light; poly(ADP-ribosyl)ation; poly(ADP-ribose) polymerase-1; cell death; apoptosis; spheroid

Introduction

Phototherapy, photochemotherapy and photodynamic therapy are efficient treatment modalities used to treat various different types of diseases ranging from psoriasis [1], acne [2] to certain forms of cancer [3] [4] [5].

Photodynamic therapy (PDT) is based on the combination of a photosensitizing compound with irradiation using a light source emitting at or near the absorption maximum of the photosensitizer [6]. In turn, the excited photosensitizer promotes the generation of oxygen radicals by directly (type I reaction) or indirectly (via intracellular substrates; type II reactions) interacting with molecular oxygen [7]. Reactive oxygen species (ROS) formed in these reactions mediate the cytotoxic effects of PDT [8].

Photochemotherapy (PCT) utilizes the combination of psoralen with suberythemogenic ultraviolet A (PUVA) [9]. Psoralens are tricyclic furocoumarins [10] with 5- methoxypsoralen (5-MOP), 8-methoxypsoralen (8-MOP) and trioxalen (TMP) being the most commonly used sensitizers [11]. Photochemical interaction between psoralens and DNA may follow three pathways: *a)* intercalation of psoralen into DNA (it may also take place without UV radiation); *b)* formation of 3,4-monoadducts or 4,6-monoadducts with the latter being capable of crosslinking psoralen with DNA following the absorption of a second photon; *c)* excited psoralen may directly react with molecular oxygen leading to the generation of singlet oxygen as in PDT [12].

PCT or PDT trigger DNA damage either directly or via ROS generation [13] [14]. The cellular response to DNA strand breaks caused by ROS or by the nucleotide excision repair pathway involves the activation of poly(ADP-ribose) polymerase-1 (PARP-1). PARP-1 is a DNA nick sensor enzyme that is abundantly expressed by most eukaryotic cell types [15] [16] [17]. Upon binding to broken DNA ends, PARP-1 becomes activated and modifies itself and nearby proteins with NAD-derived ADP-ribose. By cleaving more NAD molecules and attaching their ADP-ribose moieties to the protein proximal ADP-ribose unit, PARP-1 creates

a long, branched poly(ADP-ribose) (PAR) polymer that is essential for the recruitment of various adapter and effector DNA repair proteins [18].

From its role in DNA repair follows the plausible assumption that PARP-1 can be considered as a “survival enzyme”. Indeed, inhibition of its activity (or silencing of its expression) sensitizes cells (e.g., cancer cell lines) to subtoxic doses of ionizing radiation [19], DNA alkylating agents [20] or topoisomerase [21] inhibitors. In fact, the clinical value of such sensitization therapy has been tested in various promising clinical trials suggesting that certain tumors can indeed be eradicated more efficiently if DNA damaging chemotherapeutics are combined with PARP inhibitors [22] [23]. It may be worth mentioning here that PARP-1 inhibition/silencing/knockout may also protect cells from programmed necroptotic cell death (e.g., under conditions of severe oxidative stress) [24]. Thus, depending on the intensity of the genotoxic stimulus PARP-1 may act as a dual regulator of cell fates [16].

In a previous study from our group we reported a surprising photosensitizing effect of the PARP inhibitor PJ-34 in UVA-irradiated keratinocytes [25]. This has prompted us to investigate whether PARylation represents a possible target in PCT and whether efficiency of PCT can be improved by targeting PARP-1. It appears that while targeting PARP-1 is not likely to enhance the efficiency of PCT, one of its most widely used inhibitor PJ-34 sensitizes tumor cells to the toxic effects of UVA. Interestingly, however, the photosensitizing effect of PJ-34 is unrelated to its PARP inhibitory property.

1. Materials and Methods

1.1. Cell culture

The human epidermoid carcinoma cell line A431 (European Collection of Cell Cultures) was cultured in Dulbecco’s modified Eagle’s medium with high glucose supplemented with 10% heat-inactivated fetal bovine serum (Sigma- Aldrich, St. Louis, MO), 5% penicillin-streptomycin and 5%, L-glutamine (Lonza, Basel, Switzerland). Cells were maintained at 37°C in a humidified atmosphere (5% CO2), and were split at 70-80% confluency after trypsinization

with trypsin-EDTA solution (Sigma- Aldrich, St. Louis, MO). Cultures at 80-95% confluency were used in all experiments.

1.2. Spheroid culture

We grew spheroids from A431 cells in 96 well plates pre-coated with 0.5% agar-water solution. Cells were seeded onto plates at $1x10^4$ cells/ml density in 50 µl cell suspension per well. The cells were allowed to clump together for 48 h and were then pretreated with PARP inhibitors (PJ-34 and Veliparib) for 50 min. Cells were irradiated with UVA (2.5 J/cm^2) as described below. Immediately after irradiation, the medium was changed to fresh cell culture medium and spheroids were incubated for 16 h. Pictures of spheroids were taken with a Leica confocal microscope system. Diameter of spheroids was measured with Image J software.

1.3. Cell treatment and UVA irradiation

In all experiments the cells were pretreated for 50 min with the photosensitizer 0.8 µM 8-methoxypsoralen (8-MOP) or with PARP inhibitors, 10 µM PJ-34 (Inotek Corporation, Beverly, MA) or 10 µM Veliparib (Selleck Chemicals, Munich, Germany). In assays involving antioxidants, 200 µM Trolox (Sigma- Aldrich, St. Louis, MO) or 500 µM ascorbic acid (Sigma-Aldrich, St. Louis, MO) were added to the cultures together with the PARP inhibitors. Following pretreatment the cells were irradiated with UVA (2.5 -10 J/cm^2) in the presence or absence of PARP inhibitors in plates of uniform depth (0.109 cm in 96 well plate and 24 well plate) of phosphate-buffered saline (PBS) (0.2 M, pH 7.4). The cells were irradiated with a Bio-Sun microprocessor-controlled UV irradiation system (Wilber Lourmat, Marne-la-Vallée, France). The equipment operates at wavelength 365 nm (UVA): After irradiation PBS was replaced with fresh cell culture medium.

1.4. Cell viability assay

Cell viability was determined with MTT assay at indicated time points after irradiation [26].

1.5. Detection of reactive oxygen species

A431 cells were seeded into 96 well plates one day before the experiments. Cells were incubated for 50 min with 10 µM 2',7'-dichlorodihydrofluorescein diacetate (Sigma-Aldrich, St. Louis, MO), (In preliminary experiments we have established that in a cell-free system UVA irradiation does not activate H_2DCFDA and increased fluorescence could not be detected in UVA-irradiated H_2DCFDA solution.). Fluorescence was detected with a Fluoroskan Ascent FL plate reader (Thermo Scientific, Vantaa, Finland) immediately after UVA irradiation (ex. 480 nm, em. 590 nm).

1.6. Gene silencing

A431 cells were transfected in suspension (after trypsinization and prior to seeding). SiGENOME SMARTpool siRNA specific for human PARP-1 sequence, ON-TARGET plus Control siRNA and DharmaFECT 2 transfection reagent were obtained from Dharmacon Research, Inc. (Lafayette, CO) and silencing was carried out according to the manufacturer's instruction. After 48 h, efficiency of silencing was determined from 24-well plates by Western blotting and cells in 96-well plates were used for the viability assay 16 h after irradiation with different doses of UVA (2.5-10 J/cm^2).

1.7. Western-blotting

Antigens were detected by Western blotting according to standard procedures as described previously [27]. Antibodies specific for PAR (primary antibody: clone 10H), PARP-1, H2AX/gamma-H2AX, cleaved-PARP-1 were purchased from Cell Signaling Technology Inc. (Danvers, MA)

1.8. Immunostaining for γ-H2AX

Cells were irradiated with 5 J/cm^2 UVA for 30 min, then fixed (4% PFA for 20 min) and permeabilized (0.2% Triton X-100 in PBS buffer for 15 min). After washing, cells were blocked for one hour with 20% FCS in PBS buffer. Labeling with anti-γ-H2.AX antibody (Cell Signaling Technology, Danvers, MA) was performed overnight at 4^{o}C. Samples were washed three times with PBS and then incubated for 45 min with the peroxidase-conjugated secondary antibody (Envision, Dako). Color was developed with the chromogen DAB (3,3'-diaminobenzidine) substrate. After mounting, samples were viewed and imaged with a LeicaTCS SP8 confocal microscope. Foci were evaluated in Image J with Focinator extension [28].

1.9. Comet assay

Single-stranded DNA breaks were detected by alkaline comet assay (single-cell gel electrophoresis) as described previously [29].

1.10. Caspase activity assay and DNA fragmentation

Cells were harvested 4, 8, 16 h after irradiation, washed 1x with PBS and were lysed in lysis buffer [10 mM HEPES, 0,1% CHAPS, 5 mM dithiothreitol, 2 mM EDTA, 1 mM proteinase-inhibitor cocktail (Sigma-Aldrich, St. Louis , MO), 1 mM PMSF, pH 7.25]. Cell lysate and fluorogenic substrates [aminomethylcoumarin-conjugated caspase-3- and caspase–8- specific peptides (Ac-DEVD-AMC for caspase-3 and Ac-VETD-AMC for caspase-8; Sigma- Aldrich, St. Louis, MO)] were mixed in caspase reaction buffer (for caspase-3: 100 mM HEPES, 10% sucrose, 5 mM dithiothreitol, 0,1% CHAPS pH 7.25; for caspase-8: 75 mM Na^+ MOPS, 10% glycerol, 1 mM dithiothreitol, 0.25 mM EDTA pH 7.5). Aminomethylcoumarine (AMC) liberation was detected after 1 h incubation at 37°C using a Fluoroskan Ascent FL plate reader (Thermo Scientific, Vantaa, Finland) with excitation at 355 nm and emission at 460 nm.

Internucleosomal DNA fragmentation was detected 4, 8, 16 h after UVA irradiation (2.5 J/cm^2) by agarose gel electrophoresis as described previously [30].

1.11. [^{3}H]-NAD Incorporation Assay

The PARP activity assay was carried out as described previously [31].

1.12. Immunofluorescent staining for PAR

PAR polymer was detected by immunocytochemistry as described previously [26], except that fluorescence detection (AlexaFluor488-conjugated anti-mouse IgG antibody; Life Technologies, Budapest, Hungary) was used instead of peroxidase-labeled secondary antibody and nuclei were stained with TO-PRO-3 dye (Thermo Scientific, Vantaa, Finland). Samples were viewed and imaged with a Leica TCS SP8 confocal microscope.

1.13. Spectroscopy

Absorption spectrum of PJ-34 (dissolved in PBS) was measured with a Thermo Scientific Multiskan GO UV/VIS spectrophotometer. The NMR measurements were performed at 298 K on a Bruker AVANCE II spectrometer operating at 500.13 MHz proton resonance frequency. PJ34 (1 mg) was dissolved in 500 μl DMSO-d6 in order to make all proton signals - including those of exchangeable NH- and OH-protons as well - detectable.

1.14. Statistical analysis

All experiments were performed at least three times on different days. All the values shown in the figures are expressed as mean±S.E.M. of n observations where n represents the number of observations. Intergroup comparisons involved one-way ANOVA followed by Tukey's test. A p-value less than 0.05 was considered as significant.

2. Results

2.1. Silencing PARP-1 in A431 cells

In order to investigate the role of PARP-1 in photochemotherapy, we chose A431 skin carcinoma cells (a common model cell line in PCT research [32]) and tried to silence PARP-1 expression using siRNAs. The silencing efficiency of siRNAs in A431 cells was confirmed by a dual approach. On the one hand, we have detected PARP-1 protein levels by Western blotting, thus proving efficient gene silencing (Fig.1A). We have also used a functional test by treating cells with H_2O_2 in order to induce DNA breakage and detected poly(ADP-ribose) formation as a sign of PARP-1 activation. This latter approach also confirmed that our siRNA treatment was effective as PAR polymers could not be detected in H_2O_2-treated cells when PARP-1 was silenced (Fig.1B).

2.2. PARP-1 is not a key regulator of PUVA-induced cytotoxicity

Next, we determined the UVA sensitivity of A431 cells by irradiating them with different UVA doses (2.5–10 J/cm^2) and determining the viability of cells at 16 h after irradiation (Fig. 2A). Based on these results, we chose the 2.5 J/cm^2 UVA dose for subsequent experiments as it had no significant toxic effect on the cells (Fig. 2A) even after 48 h incubation (data not shown). In order to set up a photodynamic model we chose the photosensitizer compound 8-methoxypsoralen (8-MOP) and pretreated the cells with the photosensitizer prior to irradiation with the non-toxic UVA dose (2.5 J/cm^2). The combination of photosensitizer concentration and UVA dose was selected so that their combination cause a near 50% drop in viability in order to allow detection of further sensitization or protection by PARP-1 silencing (Fig. 2B). Interestingly, however, silencing PARP-1 had no significant effect on cell viability in this photochemotherapeutic cell death model.

2.3. The PARP inhibitor PJ-34 acts as a photosensitizer

In order to further confirm that PARP-1 is not an important regulator of cell death in PUVA-induced cytotoxicity, we also used two common PARP inhibitors PJ-34 and Veliparib. Cells were pretreated for 50min with PJ-34 (10 µM) or Veliparib (10 µM) followed by either the standard irradiation protocol with 2.5 J/cm^2 UVA or (8-MOP treatment+UVA irradiation). Interestingly, PJ-34 (Fig. 2C) sensitized cells to UVA and also to UVA+8-MOP. It is noteworthy that the photosensitizing effect of PJ-34 was as potent as that of 8-MOP (Fig. 2C). In the dark control samples (cells kept in the dark without UVA radiation) PJ-34 had no toxic effect. In contrast to PJ-34, Veliparib a PARP inhibitor with comparable potency to PJ-34 (Fig. S1) had no such sensitizing effect to UVA (Fig. 2D). From the data obtained with the PARP-1 silenced A431 cells and those treated with Veliparib we concluded that PARP-1 is not a major player in PCT, but the PARP-1 independent photosensitizing effect of PJ-34 is worthy of investigation.

2.4. The photosensitizing effect of PJ-34 can also be detected in spheroids

In order to test whether or not the photosensitizing effect of PJ-34 is restricted to 2D cultures, we managed to grow spheroids from A431 cells and repeated the photosensitization experiments. We found that under special culture conditions (as detailed in the “Materials and Methods” section) A431 cells form spheroids (Fig. 3). PJ-34 sensitized cells to otherwise non-toxic UVA doses, while the structurally unrelated Veliparib had no such effect (Fig. 3). The photosensitizing effect of PJ-34 in monolayers as well as in spheroids was also confirmed in an independent laboratory (Juarranz laboratory, Universidad Autónoma of Madrid; Fig. S2).

2.5. The phototoxic effect of PJ-34 is not suppressed by antioxidants

ROS are considered as central mediators of UVA toxicity [33]. Therefore, we have investigated whether or not PJ-34 augments ROS production and to what extent this may explain the photosensitizing effect of the compound. We detected ROS production using the ROS-sensitive fluorescent dye CM-H2DCFDA (Fig. 4) and in control experiments we ruled out false positive results caused by UVA-induced photooxidation of the probe. (Photooxidation

could be observed only at UVA doses higher than 20 J/cm^2; data not shown). Moreover, we found that the antioxidants Trolox and ascorbic acid could not prevent phototoxicity of PJ-34+UVA (Fig. 4A) despite efficiently scavenging UVA or PJ-34+UVA-induced ROS production (Fig. 4A, B). We have also tested the cytoprotective effects of additional antioxidants such as the cell-permeable antioxidant enzymes PEGylated-Catalase (PEG-CAT), PEGylated-superoxide dismutase (PEG-SOD), glutathione (GSH), and gallotannin. These antioxidants either lacked any significant effect (PEG-CAT, GSH, gallotannin) or even sensitized cells further to PJ-34+UVA-induced cytotoxicity (PEG-SOD). Moreover, the fact that ROS production was significantly but not dramatically higher in PJ-34-UVA-treated cells compared to UVA-irradiated cells (Fig. 4B) may also raise the possibility that the photosensitizing effect of PJ-34 is not due to increased ROS production. However, definitive conclusions regarding the exact role of ROS species in this model cannot be drawn from data obtained with antioxidants and this issue may require further investigation.

2.6. DNA damage accompanies the photogenotoxic effect of PJ-34

In order to better understand the mechanism of the photosensitizing effects of PJ-34 in UVA-irradiated A431 cells, next we determined DNA damage in the irradiated cells. We found that at this subtoxic UVA dose no obvious sign of DNA strand breakage could be revealed with the alkaline single cell gel electrophoresis assay (comet assay) (Fig. 5A). However, in the presence of PJ-34, marked DNA breakage could be observed both immediately and 1 h after UVA treatment, which was absent in Veliparib-pretreated cells.

Moreover, detection of phosphorylated H2AX histone variant (γH2AX) is a commonly used indicator of DNA damage triggered by photosensitizers [34]. We found γH2AX accumulation in PJ-34-pretreated and UVA-irradiated cells while the applied UVA dose alone or in combination with Veliparib had no such effect (Fig. 5B). In summary, of these two experiments it can be stated that DNA damage occurs in the presence of PJ-34 if cells are exposed to a subtoxic dose of UVA. In the timeframe, the investigated DNA damage proved stable.

2.7. UVA-irradiated A431 cells die by apoptosis in the presence of PJ-34

In order to characterize the cell death induced by PJ-34+UVA treatment, apoptotic parameters were investigated. We found that 4 h after irradiation caspase-3, a central executioner of apoptosis is activated in UVA irradiated cells if PJ-34 is present (Fig. 6A), whilst Veliparib had no such effect. In the PJ-34+UVA-treated samples caspase activity was further enhanced at 8 h and the activity was sustained even 16 h after irradiation. Increased caspase-3-like activity was also evidenced by detecting PARP-1 cleavage (PARP-1 was one of the first described substrates of caspase-3). The 89 kDa cleavage product of PARP-1 was detectable at 4 h after irradiation with its abundance increasing even further at 8 h and 16 h (Fig. 6B). Activation of caspase-8, an initiator caspase of the extrinsic apoptotic pathway could also be detected as early as 4 h after irradiation with further significant increases at 8 h and 16 h (Fig. 6C). The active role of caspases in the cell death process initiated by PJ-34+UVA treatment is supported by our observations that the pan-caspase inhibitor z-vad-fmk, the caspase-3 inhibitor z-DEVD-fmk as well as the caspase-8 inhibitor z-IETD-fmk protected A431 cells from the toxicity (Fig. 6D). In the course of apoptosis, effector caspases unleash the DNA fragmentation machinery. Internucleosomal DNA fragmentation could also be detected in our UVA irradiation model but only in the presence of PJ-34 and not in the presence of Veliparib (Fig. 7). A marked necrotic component could not be seen to accompany apoptosis.

3. Discussion

Although PDT and PCT differ in their applications as well as mechanism of action [3], both methods rely on the cytotoxic combination of a photosensitizer with light of matching wavelength [35]. While in PCT cellular events that are triggered by DNA damage which may induce secondary generation of reactive oxygen species, in PDT production of ROS is a primary event causing secondary oxidative DNA damage [5] as well as membrane damage

[36], activation of the immune system [37] [38], inhibition of cell proliferation [39] and vascularization [40].

Current aims of PDT- and PCT-related research focus on improving equipment and the delivery of activating light, increasing the tumor specificity of the treatment and developing novel, more powerful sensitizer compounds [41]. The current paper investigates the potential role of PARylation in photosensitization which fits this latter trend.

PARP-1 has already been implicated in the repair of UVC-induced DNA damage via the nucleotide excision repair (NER) pathway [42], its role in PUVA lesion repair has not yet been investigated. Thus, the primary aim of our study was to investigate the role of PARylation in the response of the cells to PUVA treatment. Our original hypothesis was that by inhibiting the repair of PUVA-induced DNA damage, PARP inhibition would sensitize cells to UVA light. Somewhat surprisingly, this hypothesis had to be rejected because both PARP-1 silencing and PARP inhibition by the specific and potent PARP inhibitor Veliparib (which is now in phase III clinical trial for the treatment of HER-2 negative breast cancer associated with BRCA mutations [43]) failed to sensitize cells to the toxic effects of PUVA or to low dose UVA radiation. The compound was not inactivated by the applied UV dose (Suppl. Fig S1), therefore, it seems that PARylation is not of vital importance for the repair of PUVA photoproducts and cannot be considered as a crucial survival mechanism in PUVA-treated cells.

Interestingly, however, PJ-34 is a PARP inhibitor with similar or somewhat lower potency than Veliparib that did sensitize the cells to UVA both in 2D cultures and in spheroids. One peak in the absorption spectrum of PJ-34 overlaps with the emission spectrum of the UVA irradiator used in this study raising the possibility that the compound can absorb UVA light. Moreover, it appears likely that UVA irradiation triggers a structural change in the PJ-34 molecule as indicated by the altered absorption spectrum and NMR spectrum of the compound recorded before and after UVA irradiation (Fig. S3). Based on the new resonance signals appearing in the aromatic (7-9 ppm) and phenolic -OH (11-11.5 ppm) regions, tautomers (ca. 20-30% of PJ-34) with extended conjugated pi-electron system are likely to be formed (Fig. S3C).

The fact that the sensitizing effect of PJ-34 could be observed both in 2D and in 3D cultures is important because 3D spheroid cultures represent a “microtumor” and this model has been used with increasing frequency to evaluate photosensitizing agents [44] as spheroids more closely model nutrient supply, oxygenation, pH inhomogeneities than traditional 2D cultures. Similar sensitivity of cells to PJ-34+UVA in 2D as well as in 3D cultures provides support for confirming this effect also in *in vivo* animal models.

Further characterization of the effects of PJ-34 revealed that the compound slightly increases UVA-induced ROS production and dramatically enhances DNA damage. Somewhat surprisingly, the antioxidants trolox or ascorbic acid (and several other antioxidants) failed to prevent photosensitization by PJ-34 despite efficiently scavenging UVA-induced or PJ-34+UVA-induced ROS production. It must be noted here, however, that the data in the literature on the effects of various antioxidants are rather controversial with reports on ascorbic acid or trolox (the antioxidants used in our study) ranging from protection, to lack of effect or even potentiation of PDT phototoxicity [45-48]. The key to understanding this controversy may lie in differences in the severity of the PDT/PCT model, the cell type, the concentration and cellular/subcellular penetration of the photosensitizer, concentration of the antioxidants and various other variables of the biological models used in these studies.

Two types of regulated cell death pathways (apoptosis and necrosis) have been shown to be induced by the interaction of light and photosensitizers [49] [32]. PCT-induced DNA damage triggered apoptotic cell death characterized by caspase activation and internucleosomal DNA fragmentation [34]. As for the caspases, both caspase-3 and caspase-8 were activated in PJ-34+UVA-treated cells. Activation of caspase 8 may indicate that PCT treatment activated the extrinsic apoptotic pathway (e.g., via FAS signaling). Previous reports [50] showing the involvement of this route in PCT may support this scenario [51]. Alternatively, caspase-8 activity may also result from activation of the caspase-3-caspase-6 axis downstream of apoptosome formation [52] [53]. Which of these two options may be relevant and what the hierarchy of caspases is in our model, requires further investigation. No sign of necrosis could

be seen in our model, thus necrosis does not appear to be the major pathway of cell death in PJ-34-sensitized and UVA-irradiated A431 cells.

As for the practical implications of our findings, it appears plausible to suggest that PJ-34 may be worth investigating as a novel photosensitizer with potential applications in PDT or in PCT. However, several open questions remain to be answered before PJ-34 may enter the path of translation. Its photosensitization effect must be characterized in more detail and various different types of cancer cell lines should be tested for sensitivity to PJ-34+UVA treatment. Furthermore, the *in vivo* efficiency of the compound should also be verified.

Acknowledgements

This research was supported by the European Union and the State of Hungary, and co-financed by the European Social Fund in the framework of TÁMOP 4.2.4.A/2-11/1-2012-0001 'National Excellence Program'. The direct costs of this study were supported by the Hungarian Science Research Fund to L.V. (OTKA K112336) and to C.H. (OTKA PD116845), by MINECO (FIS PI12/01253), and Comunidad de Madrid (S2010/BMD-2359) to A.J.

Conflict of interest: Authors declare no conflict of interest.

Legends of figures

Figure 1. Silencing of PARP-1 by siRNA

PARP-1 expression was suppressed in A431 cells by siRNA. **(A)** Efficiency of silencing was confirmed by Western-blot analysis using a PARP-1 specific antibody. **(B)** In order to functionally characterize the effect of silencing, the cells were treated with 1 mM hydrogen-peroxide and PAR production was detected by immunoblotting (TR control: DharmaFECT transfection reagent without siRNA; siCTL: transfected with non-target control siRNA; siPARP-1: transfected with PARP-1-specific siRNA). In both cases ß–actin was used as loading control. Intensity of the bands was quantified by densitometry. Star symbol represents a statistically significant (*$p<0.05$) difference between A431 control cells and PARP-1 silenced cells on panel A or between H_2O_2 unexposed and exposed cells on panel B. Hashtag symbol indicates statistically significant (#$p<0.05$) difference in PAR accumulation between siCTL+ H_2O_2 and siPARP-1 + H_2O_2.

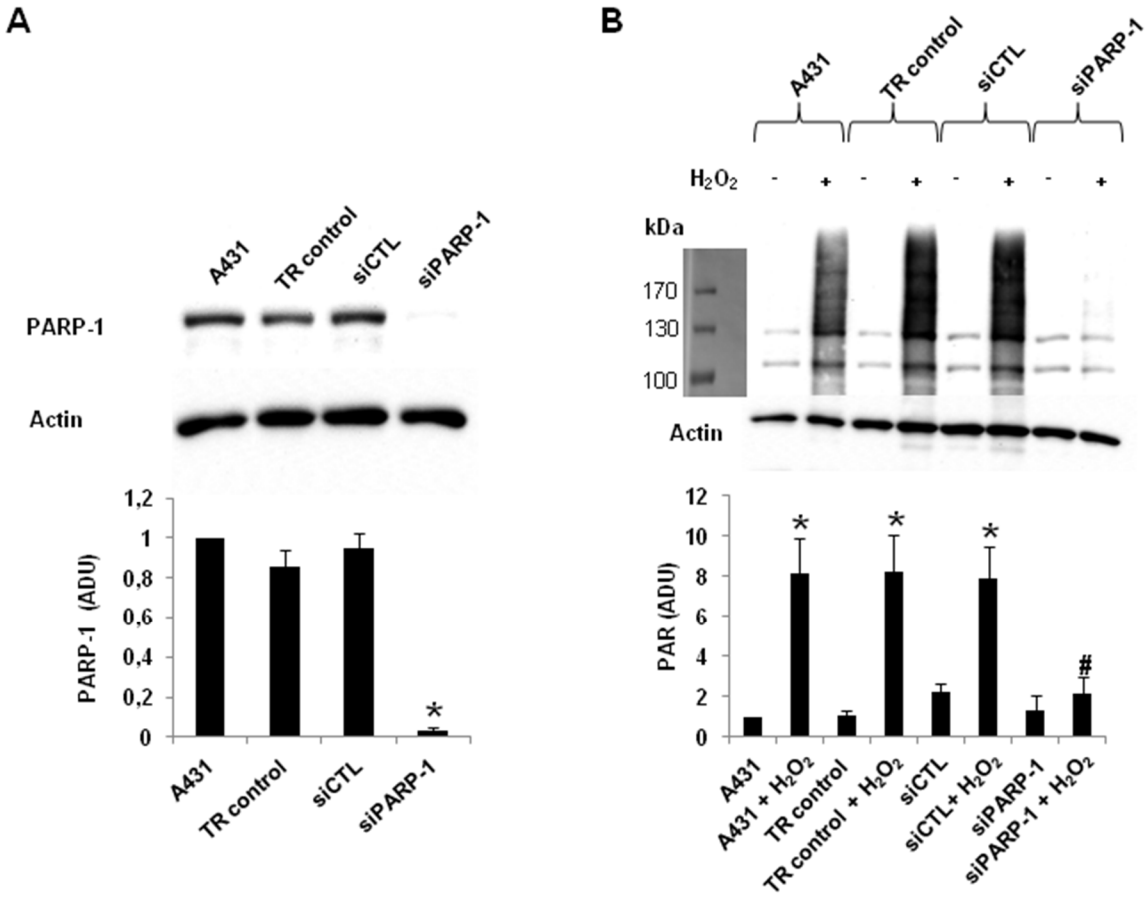

Figure 1.

Figure 2. PARP-1 is not a key regulator of PDT but PJ-34 acts as a photosensitizer independently of its PARP inhibitory effect (A) The hypothesized potentiating effect of

PARP-1 silencing to UVA was tested by comparing the effects of PARP-1 silencing (siPARP-1) to non-target siRNA (siCTL) or transfection reagent only (TR). Viability of cells was measured 16 h after UVA irradiation (2.5 – 10 J/cm^2) with MTT assay. **(B)** Phototoxic effect of 8MOP+UVA (2.5 J/cm^2) on PARP-1 silenced A431 cells was measured in MTT assay 16 h after irradiation. **(C)** Effect of PJ-34 on 8MOP+UVA-induced cell death and **(D)** photosensitizing effect of PJ-34 compared to another potent PARP inhibitor Veliparib were determined in MTT assay at 16 h after UVA irradiation (2.5 J/cm^2). Data on panels represent mean±S.E. of three independent experiments. Star symbol represents statistically significant (*$p<0.05$) difference between dark control cells and 8MOP+UVA-treated cells (B) or phototoxic effect of PJ-34 and 8MOP (C and D). Hashtag symbol indicates statistically significant (#$p<0.05$) sensitization by PJ-34 compared to 8MOP+UVA (C) or UVA (D).

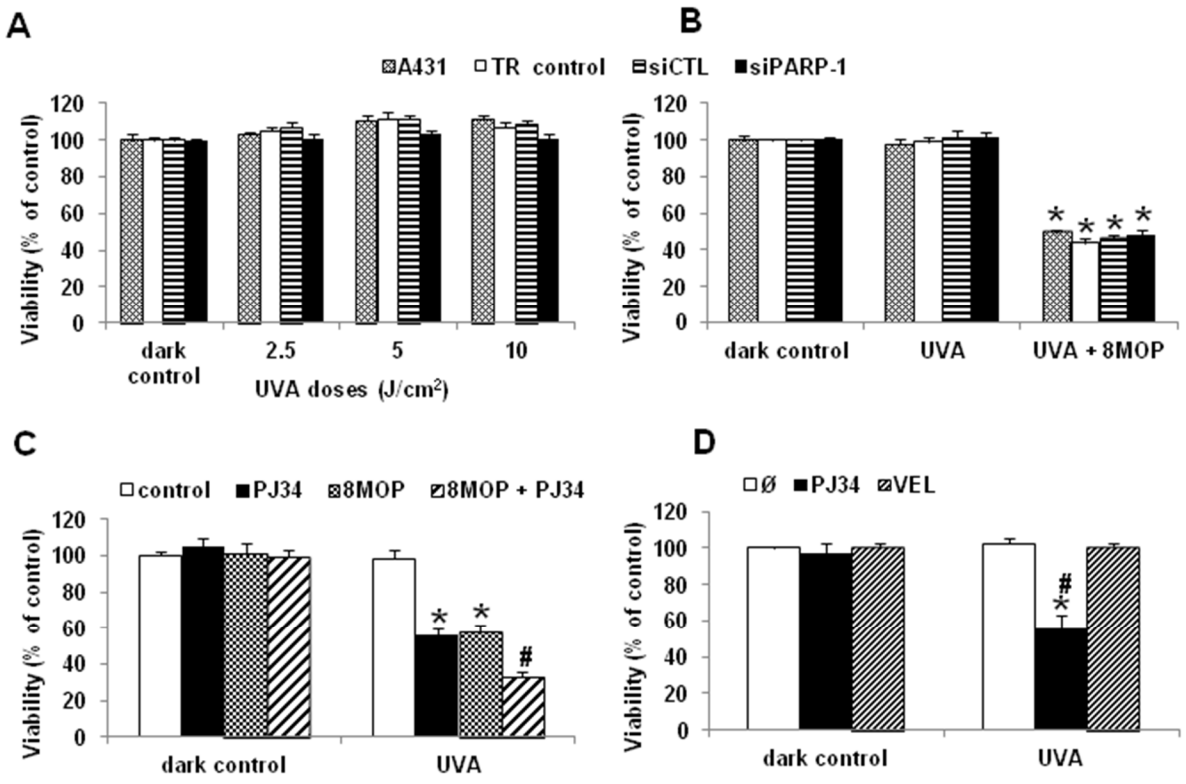

Figure 2.

Figure 3. Chemical phototoxicity of PJ-34 in spheroid cultures

A431 spheroids were either left in the dark or were irradiated with 2.5 J/cm^2 UVA in the presence of two PARP inhibitors PJ-34 (10 µM) or Veliparib (10 µM). Diameters were

measured 16 h after irradiation. Scale bar is 200 μm. Data on panels represent mean±S.E. of three independent experiments. Star symbol represents statistically significant (*$p<0.05$) difference between dark control and UVA irradiated cells. Hashtag symbol indicates statistically significant (#$p<0.05$) difference between UVA-irradiated and PJ-34+UVA-treated cells.

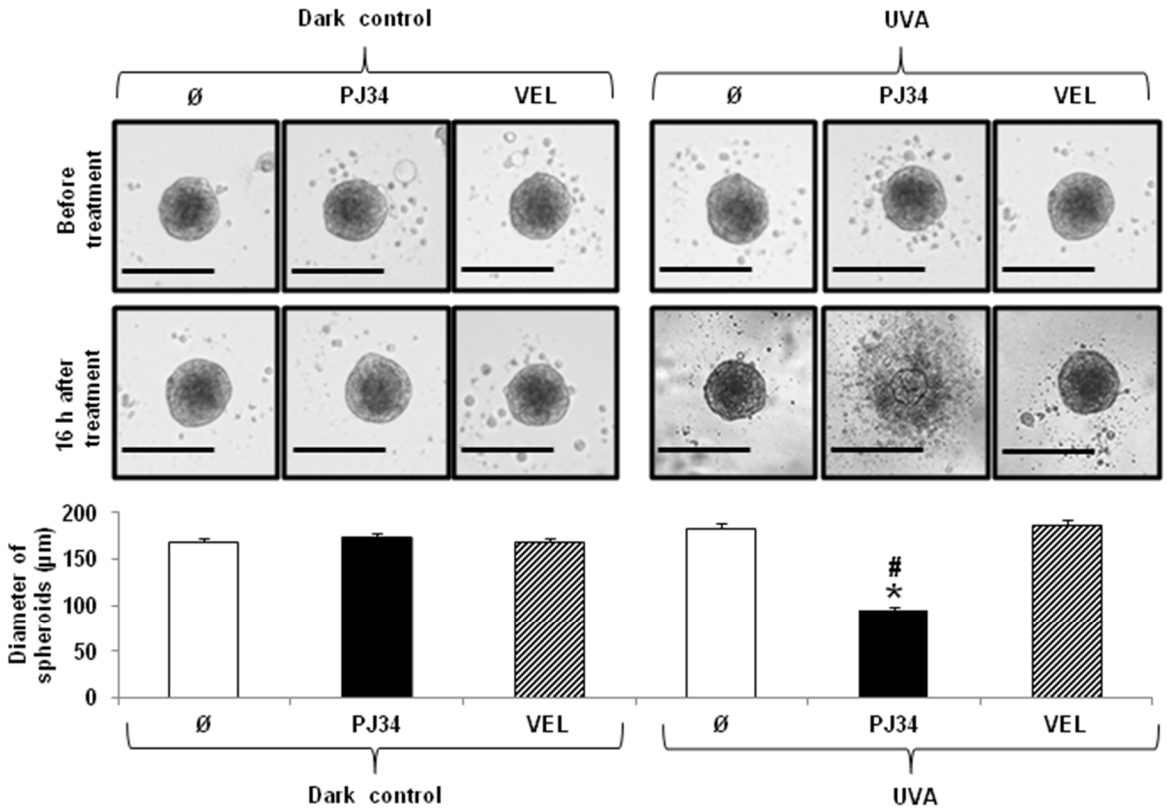

Figure 3.

Figure 4. Antioxidants do not prevent UVA+PJ-34 induced phototoxicity despite efficiently scavenging ROS

A431 cells were either left in the dark or irradiated with 2.5 J/cm^2 UVA in the presence of two PARP inhibitors PJ-34 (10 µM) or Veliparib (10 µM). Cell viability was measured with MTT assay 16 h after irradiation. The effects of the antioxidants trolox (200 µM) or ascorbic acid (500 µM) were tested on the viability **(A)** at 16 h or ROS production **(B)** (immediately after UVA irradiation). Data on panels represent mean±S.E. of three independent experiments. Star symbol represents statistically significant (*$p<0.05$) difference between dark control and UVA-irradiated cells. Hashtag indicates statistically significant (#$p<0.05$) difference between UVA-irradiated and PJ-34+UVA-treated cells. Dollar symbol indicates statistically significant ($p<0.05$) effect of antioxidants.

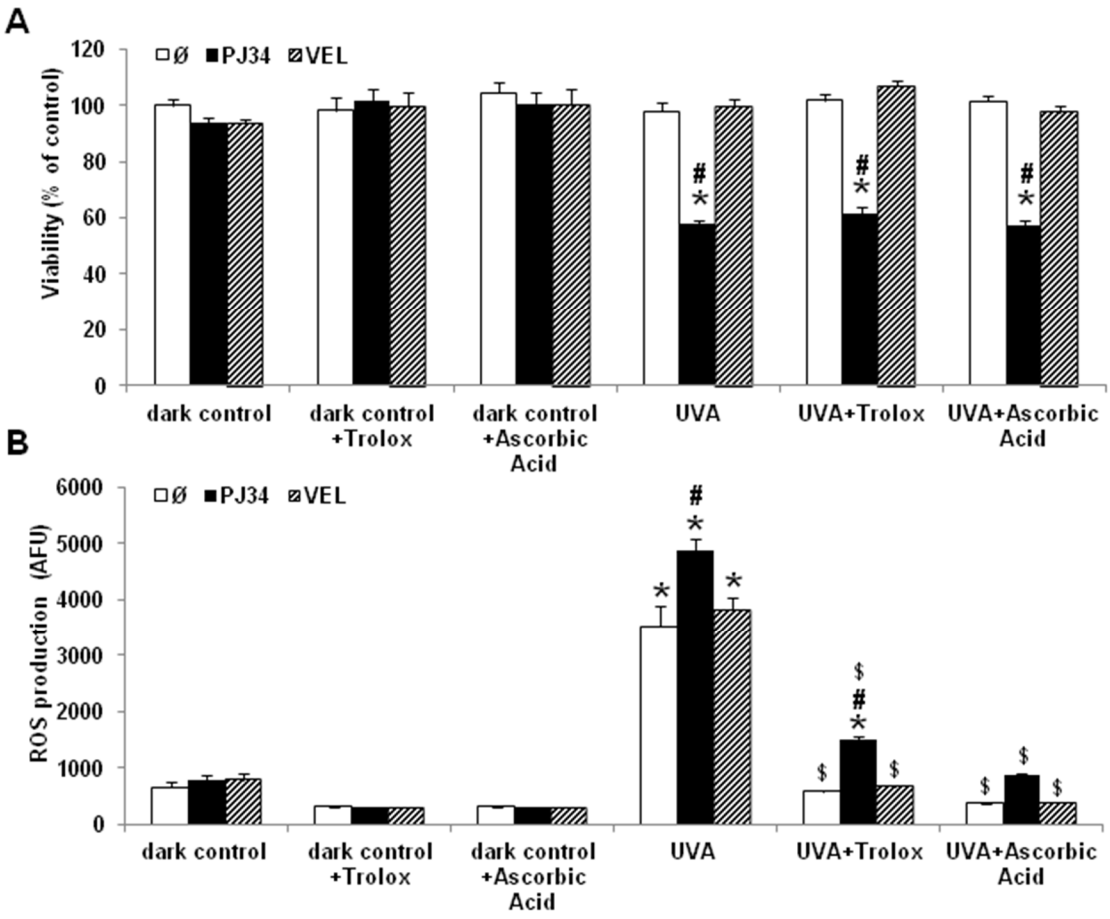

Figure 4.

Figure 5. PJ-34 + UVA causes DNA damage

(A) DNA single strand breaks were detected in alkaline Comet assay in the dark control cells and immediately or 1 h after UVA irradiation in the presence or absence of PARP inhibitors

PJ-34 (10 µM) or Veliparib (10 µM). Values of olive tail moment were used for quantitative analysis of DNA damage. Original magnification was 63x. Scale bar is 25 µm. **(B)** DNA double strand breaks were assessed by detecting γ-H2AX in the dark control cells or at indicated times after UVA irradiation (2.5 J/cm^2) in the presence or absence of PARP inhibitors PJ-34 or Veliparib (10 µM). Intensity of the bands was quantified by densitometry. Data on panels represent mean±S.E. of three independent experiments. Star symbol represents statistically significant (*$p<0.05$) difference between dark control and UVA irradiated cells. Hashtag symbol indicates statistically significant (#$p<0.05$) effect of PJ-34 compared to UVA-exposed samples.

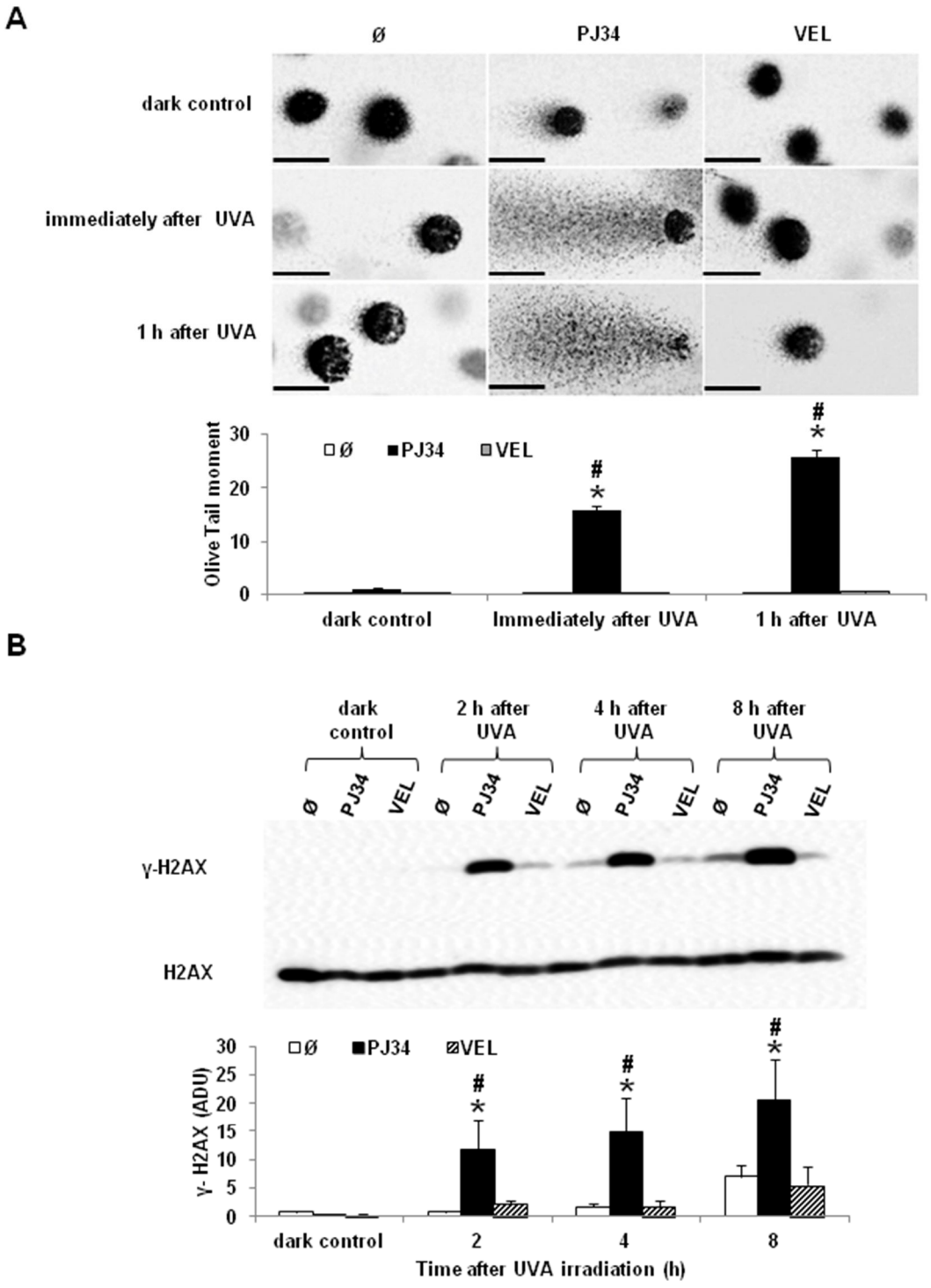

Figure 5.

Figure 6. Photogenotoxic effect of PJ-34 triggers apoptotic cell death.

(A) Caspase-3 and **(C)** caspase-8 activities were measured in dark control cells or at indicated times after UVA irradiation (2.5 J/cm^2) in the presence or absence of the PARP inhibitors PJ-

34 (10 µM) or Veliparib (10 µM). **(B)** PARP-1 cleavage was detected by immunoblotting in dark control cells or after UVA irradiation in the presence or absence of the PARP inhibitors PJ-34 or Veliparib (10 µM) at indicated time points. ß–actin was used as loading control. Intensities of the bands were quantified by densitometry. **(D)** Protective effect of caspase inhibitors on cell viability was measured with MTT assay 16h after UVA irradiation (2.5 J/cm^2) in the presence or absence of PARP inhibitors PJ-34 or Veliparib (10 µM) or in dark control cells. Data on panels represent mean±S.E. of three independent experiments. Star symbol represents statistically significant (*$p<0.05$) difference between dark control and UVA irradiated cells. Hashtag symbol indicates statistically significant (#$p<0.05$) between UVA irradiated and UVA + PJ-34 treated cells.

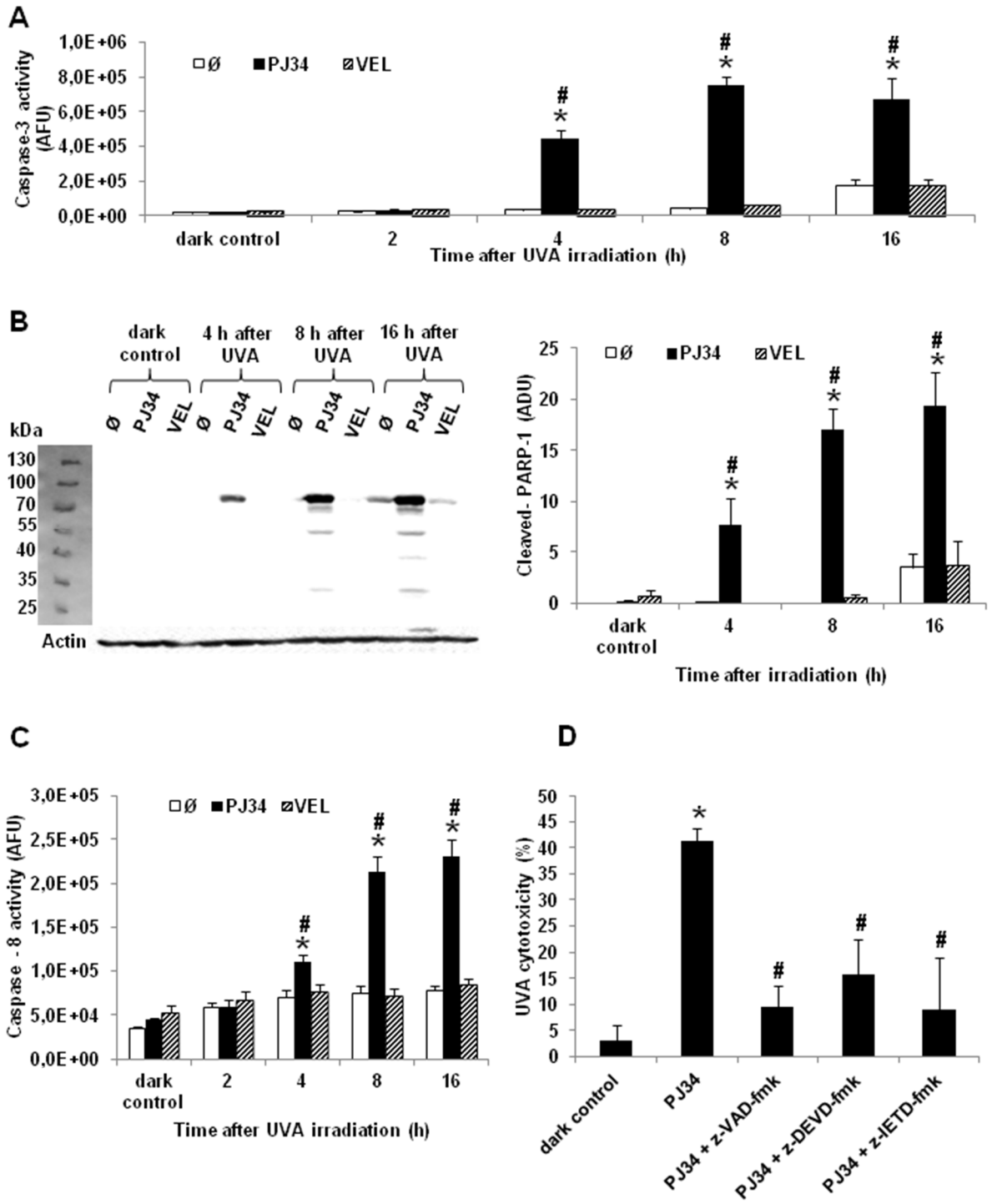

Figure 6.

Figure 7. PJ-34 + UVA treatment causes DNA fragmentation.

DNA fragmentation was detected in dark control cells or after UVA irradiation (2.5 J/cm^2) in the presence or absence of PARP inhibitors PJ-34 or Veliparib (10 µM). Intensities of the bands

were quantified by densitometry. Data in panels represent mean±S.E. of three independent experiments. Star symbol represents statistically significant (*p<0.05) difference between dark control and UVA irradiated cells. Hashtag symbol indicates statistically significant (#p< 0.05) increase in DNA fragmentation in the presence of PJ-34.

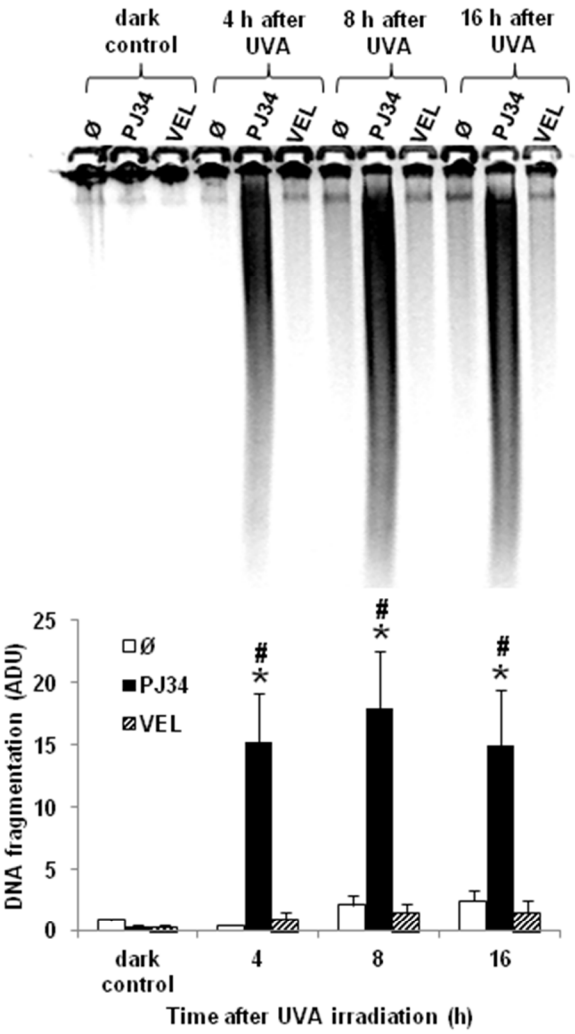

Figure 7.

Supplementary Figure S1. PJ-34 and Veliparib are similarly potent PARP inhibitors and they do not lose their inhibitory ability upon UVA irradiation

(A) A431 cells were exposed to hydrogen-peroxide (1 mM) for 7 min and PARP activation was measured in the ^{3}H-NAD-based PARP activity assay. **(B and C)** Hydrogen-peroxide- (1 mM) or UVA-induced PAR accumulation was detected by immunostaining and Western-blot analysis using a PAR-specific antibody. In the case of immunostainings (B) nuclei were counterstained with TO-PRO. Original magnification was 63x. Scale bar is 25 µm. On the immunoblots (C) ß–actin was used as a loading control and the intensity of the bands was quantified by densitometry. In all experiments, A431 cells were pretreated with two specific PARP inhibitors PJ-34 or Veliparib (in indicated concentrations) prior to the hydrogen-peroxide treatment or UVA irradiation (2.5 J/cm^2). Data on panels represent mean±S.E. of three independent experiments. Star symbol represents statistically significant (*p<0.05) effect of hydrogen-peroxide treatment. Hashtag symbol indicates statistically significant (#p<0.05) effect of PARP inhibitors on hydrogen-peroxide-induced PARP activation **(A)** or PAR accumulation **(C)**.

Supplementary Figure S2. Confirmation of spheroid data

Spheroid data presented in Figure 3 (produced in the Virag laboratory, Debrecen, Hungary) were confirmed by findings from an independent laboratory (i.e., that of Angeles Juarranz, Madrid, Spain).

A. Cellular morphology of A-431 cells (monolayer and spheroids) analyzed by phase contrast at 16 h after treatments. B. Cell survival of A-431 cells (monolayer and spheroids) measured by MTT assay at 16 h after the different treatments. (**p<0,001)

Method used to grow spheroids was different from the protocol used by the Virag laboratory. Here, 80% confluent cultures were harvested with trypsin and gently pipetted to form a single cell suspension. The cells were centrifuged at 1700 rpm for 5 min, resuspended in spheroid medium and plated in appropriated plates. Parallel control cultures were seeded in spheroid medium and grown as attached monolayers on conventional plastic plates. The spheroid medium consists of DMEM/F12 (1:1) (HyClone, Logan, Utah/Gibco, Waltham, Massachusetts) containing 2% B27 serum-free supplement (Invitrogen, Frederick, Maryland), 20 ng/ml EGF,

0.4% bovine serum albumin and 4 µg/ml insulin (Sigma, St. Louis, Missouri). The cells were plated at 40,000 cells per 9.5 cm^2 well in 1.2% poly-HEMA coated plates. Poly-HEMA was prepared by suspending 1.2 g poly-HEMA (Sigma, 2-hydroxyethyl methacrylate) per 100 ml 95% ethanol and heating at 65°C with mixing. Dishes were coated by addition of 2.5 ml of poly-HEMA stock per 9.5 cm^2 dish in a sterile hood. The ethanol was evaporated overnight and the plates were sterilized by 1 h UV irradiation (Adhikary G et al. 2013; DOI: 10.1371/journal.pone.008432). For treatments, both spheroids and attached monolayer cultures were treated for 1 h with 10 µM PJ-34, washed in PBS and subjected to UVA irradiation (2.5 J/cm^2). Cultures were evaluated morphologically by phase contrast microscopy and by MTT for measuring cell survival after treatment (16 h). Scale bar is 100 µm.

Supplementary Figure S3. UVA irradiation alters the absorption spectrum and the 1H NMR spectrum of PJ-34

The absorption spectrum of PJ-34 solution (500 µM in PBS) has been recorded with a UV/VIS spectrophotometer (A). The compound was dissolved in DMSO-d6 (1 mg/500 µl) for NMR spectroscopy (B). UV and NMR spectra were recorded both before and after irradiation with 2.5 J/cm^2 UVA. Structure of PJ-34 as well as proposed structures of UVA-induced tautomers are shown (C).

Supplementary Table S1

A431 cells were pretreated for 30 min with the indicated concentrations of the listed antioxidants followed by PJ34+UVA treatment as described in the ‘Methods’ section. Viability was determined with the MTT method and cytoprotective effects were calculated and expressed as % protection. (Negative values indicate sensitizing rather than a protective effect.) Star symbol represents statistically significant (*$p<0.05$; **$p<0.01$) cytoprotective or sensitizing effects of the treatments.

References

[1] Y.K. Tandon, M.F. Yang, E.D. Baron, Role of photodynamic therapy in psoriasis: a brief review, Photodermatol Photoimmunol Photomed, 24 (2008) 222-230.

[2] W. Zheng, Y. Wu, X. Xu, X. Gao, H.D. Chen, Y. Li, Evidence-based review of photodynamic therapy in the treatment of acne, Eur J Dermatol, 24 (2014) 444-456.

[3] L. Dalla Via, S. Marciani Magno, Photochemotherapy in the treatment of cancer, Curr Med Chem, 8 (2001) 1405-1418.

[4] M.A. Biel, Photodynamic therapy in head and neck cancer, Curr Oncol Rep, 4 (2002) 87-96.

[5] E. Ledo, A. Ledo, Phototherapy, photochemotherapy, and photodynamic therapy: unapproved uses or indications, Clin Dermatol, 18 (2000) 77-86.

[6] C.A. Robertson, D.H. Evans, H. Abrahamse, Photodynamic therapy (PDT): a short review on cellular mechanisms and cancer research applications for PDT, J Photochem Photobiol B, 96 (2009) 1-8.

[7] M. Triesscheijn, P. Baas, J.H. Schellens, F.A. Stewart, Photodynamic therapy in oncology, Oncologist, 11 (2006) 1034-1044.

[8] I. Moserova, J. Kralova, Role of ER stress response in photodynamic therapy: ROS generated in different subcellular compartments trigger diverse cell death pathways, PLoS One, 7 (2012) e32972.

[9] F. Almutawa, N. Alnomair, Y. Wang, I. Hamzavi, H.W. Lim, Systematic review of UV-based therapy for psoriasis, Am J Clin Dermatol, 14 (2013) 87-109.

[10] D.R. Bickers, H. Mukhtar, S.J. Molica, Jr., M.A. Pathak, The effect of psoralens on hepatic and cutaneous drug metabolizing enzymes and cytochrome P-450, J Invest Dermatol, 79 (1982) 201-205.

[11] M.A. Pathak, P.C. Joshi, The nature and molecular basis of cutaneous photosensitivity reactions to psoralens and coal tar, J Invest Dermatol, 80 (1983) 66s-74s.

[12] S. Couve-Privat, G. Mace, F. Rosselli, M.K. Saparbaev, Psoralen-induced DNA adducts are substrates for the base excision repair pathway in human cells, Nucleic Acids Res, 35 (2007) 5672-5682.

[13] S. Tada-Oikawa, S. Oikawa, J. Hirayama, K. Hirakawa, S. Kawanishi, DNA damage and apoptosis induced by photosensitization of 5,10,15,20-tetrakis (N-methyl-4-pyridyl)-21H,23H-porphyrin via singlet oxygen generation, Photochem Photobiol, 85 (2009) 1391-1399.

[14] R. Brem, X. Zhang, Y.Z. Xu, P. Karran, UVA photoactivation of DNA containing halogenated thiopyrimidines induces cytotoxic DNA lesions, J Photochem Photobiol B, 145C (2015) 1-10.

[15] C. Hegedus, L. Virag, Inputs and outputs of poly(ADP-ribosyl)ation: Relevance to oxidative stress, Redox Biol, 2C (2014) 978-982.

[16] L. Virag, C. Szabo, The therapeutic potential of poly(ADP-ribose) polymerase inhibitors, Pharmacol Rev, 54 (2002) 375-429.

[17] A.L. Piberger, C. Keil, S. Platz, S. Rohn, A. Hartwig, Sulforaphane inhibits damage-induced poly (ADP-ribosyl)ation via direct interaction of its cellular metabolites with PARP-1, Mol Nutr Food Res, 59 (2015) 2231-2242.

[18] L. Virag, A. Robaszkiewicz, J.M. Rodriguez-Vargas, F.J. Oliver, Poly(ADP-ribose) signaling in cell death, Mol Aspects Med, 34 (2013) 1153-1167.

[19] P. Chatterjee, G.S. Choudhary, A. Sharma, K. Singh, W.D. Heston, J. Ciezki, E.A. Klein, A. Almasan, PARP inhibition sensitizes to low dose-rate radiation TMPRSS2-ERG fusion gene-expressing and PTEN-deficient prostate cancer cells, PLoS One, 8 (2013) e60408.

[20] D.A. Loser, A. Shibata, A.K. Shibata, L.J. Woodbine, P.A. Jeggo, A.J. Chalmers, Sensitization to radiation and alkylating agents by inhibitors of poly(ADP-ribose) polymerase is enhanced in cells deficient in DNA double-strand break repair, Mol Cancer Ther, 9 (2010) 1775-1787.

[21] L.M. Smith, E. Willmore, C.A. Austin, N.J. Curtin, The novel poly(ADP-Ribose) polymerase inhibitor, AG14361, sensitizes cells to topoisomerase I poisons by increasing the persistence of DNA strand breaks, Clin Cancer Res, 11 (2005) 8449-8457.

[22] D. Nguyen, M. Zajac-Kaye, L. Rubinstein, D. Voeller, J.E. Tomaszewski, S. Kummar, A.P. Chen, Y. Pommier, J.H. Doroshow, S.X. Yang, Poly(ADP-ribose) polymerase inhibition enhances p53-dependent and -independent DNA damage responses induced by DNA damaging agent, Cell Cycle, 10 (2011) 4074-4082.

[23] A. Sonnenblick, E. de Azambuja, H.A. Azim, Jr., M. Piccart, An update on PARP inhibitors--moving to the adjuvant setting, Nat Rev Clin Oncol, 12 (2015) 27-41.

[24] X. Xu, C.C. Chua, M. Zhang, D. Geng, C.F. Liu, R.C. Hamdy, B.H. Chua, The role of PARP activation in glutamate-induced necroptosis in HT-22 cells, Brain Res, 1343 (2010) 206-212.

[25] P. Lakatos, E. Szabo, C. Hegedus, G. Hasko, P. Gergely, P. Bai, L. Virag, 3-Aminobenzamide protects primary human keratinocytes from UV-induced cell death by a poly(ADP-ribosyl)ation independent mechanism, Biochim Biophys Acta, 1833 (2013) 743-751.

[26] K. Erdelyi, P. Bai, I. Kovacs, E. Szabo, G. Mocsar, A. Kakuk, C. Szabo, P. Gergely, L. Virag, Dual role of poly(ADP-ribose) glycohydrolase in the regulation of cell death in oxidatively stressed A549 cells, FASEB J, 23 (2009) 3553-3563.

[27] K. Erdelyi, A. Kiss, E. Bakondi, P. Bai, C. Szabo, P. Gergely, F. Erdodi, L. Virag, Gallotannin inhibits the expression of chemokines and inflammatory cytokines in A549 cells, Mol Pharmacol, 68 (2005) 895-904.

[28] S. Oeck, N.M. Malewicz, S. Hurst, J. Rudner, V. Jendrossek, The Focinator - a new open-source tool for high-throughput foci evaluation of DNA damage, Radiat Oncol, 10 (2015) 163.

[29] P. Bai, C. Hegedus, K. Erdelyi, E. Szabo, E. Bakondi, S. Gergely, C. Szabo, L. Virag, Protein tyrosine nitration and poly(ADP-ribose) polymerase activation in N-methyl-N-nitro-N-nitrosoguanidine-treated thymocytes: implication for cytotoxicity, Toxicol Lett, 170 (2007) 203-213.

[30] L. Virag, D.J. Marmer, C. Szabo, Crucial role of apopain in the peroxynitrite-induced apoptotic DNA fragmentation, Free Radic Biol Med, 25 (1998) 1075-1082.

[31] G.E. Abdelkarim, K. Gertz, C. Harms, J. Katchanov, U. Dirnagl, C. Szabo, M. Endres, Protective effects of PJ34, a novel, potent inhibitor of poly(ADP-ribose) polymerase (PARP) in in vitro and in vivo models of stroke, Int J Mol Med, 7 (2001) 255-260.

[32] P. Mroz, A. Yaroslavsky, G.B. Kharkwal, M.R. Hamblin, Cell death pathways in photodynamic therapy of cancer, Cancers (Basel), 3 (2011) 2516-2539.

[33] B. Cortat, C.C. Garcia, A. Quinet, A.P. Schuch, K.M. de Lima-Bessa, C.F. Menck, The relative roles of DNA damage induced by UVA irradiation in human cells, Photochem Photobiol Sci, 12 (2013) 1483-1495.

[34] T. Toyooka, M. Ishihama, Y. Ibuki, Phosphorylation of histone H2AX is a powerful tool for detecting chemical photogenotoxicity, J Invest Dermatol, 131 (2011) 1313-1321.

[35] E.M. Nagy, L. Dalla Via, L. Ronconi, D. Fregona, Recent advances in PUVA photochemotherapy and PDT for the treatment of cancer, Curr Pharm Des, 16 (2010) 1863-1876.

[36] C. Sousa, T.S. Melo, J.C. Maziere, R. Santus, PUVA-induced cell mortality in NCTC 2544 keratinocytes: is it related to the microenvironmental properties of the excited states of psoralens?, Photochem Photobiol, 67 (1998) 561-564.

[37] J. Piette, Signalling pathway activation by photodynamic therapy: NF-kappaB at the crossroad between oncology and immunology, Photochem Photobiol Sci, (2015).

[38] P. Skupin-Mrugalska, L. Sobotta, M. Kucinska, M. Murias, J. Mielcarek, N. Duzgunes, Cellular changes, molecular pathways and the immune system following photodynamic treatment, Curr Med Chem, 21 (2014) 4059-4073.

[39] B. Cunderlikova, V. Vasovic, L.L. Randeberg, E. Christensen, T. Warloe, J.M. Nesland, Q. Peng, Modification of extracorporeal photopheresis technology with porphyrin precursors. Comparison between 8-methoxypsoralen and hexaminolevulinate in killing human T-cell lymphoma cell lines in vitro, Biochim Biophys Acta, 1840 (2014) 2702-2708.

[40] Z. Zhen, W. Tang, Y.J. Chuang, T. Todd, W. Zhang, X. Lin, G. Niu, G. Liu, L. Wang, Z. Pan, X. Chen, J. Xie, Tumor vasculature targeted photodynamic therapy for enhanced delivery of nanoparticles, ACS Nano, 8 (2014) 6004-6013.

[41] D.E. Dolmans, D. Fukumura, R.K. Jain, Photodynamic therapy for cancer, Nat Rev Cancer, 3 (2003) 380-387.

[42] M. Robu, R.G. Shah, N. Petitclerc, J. Brind'Amour, F. Kandan-Kulangara, G.M. Shah, Role of poly(ADP-ribose) polymerase-1 in the removal of UV-induced DNA lesions by nucleotide excision repair, Proc Natl Acad Sci U S A, 110 (2013) 1658-1663.

[43] C. Guillot, V. Favaudon, Z. Herceg, C. Sagne, S. Sauvaigo, P. Merle, J. Hall, I. Chemin, PARP inhibition and the radiosensitizing effects of the PARP inhibitor ABT-888 in in vitro hepatocellular carcinoma models, BMC Cancer, 14 (2014) 603.

[44] C. Dubessy, J.M. Merlin, C. Marchal, F. Guillemin, Spheroids in radiobiology and photodynamic therapy, Crit Rev Oncol Hematol, 36 (2000) 179-192.

[45] S. Grimm, D. Mvondo, T. Grune, N. Breusing, The outcome of 5-ALA-mediated photodynamic treatment in melanoma cells is influenced by vitamin C and heme oxygenase-1, Biofactors, 37 (2011) 17-24.

[46] A. Bernd, Visible light and/or UVA offer a strong amplification of the anti-tumor effect of curcumin, Phytochem Rev, 13 (2014) 183-189.

[47] R. Yin, M. Wang, Y.Y. Huang, G. Landi, D. Vecchio, L.Y. Chiang, M.R. Hamblin, Antimicrobial photodynamic inactivation with decacationic functionalized fullerenes: Oxygen-independent photokilling in presence of azide and new mechanistic insights, Free Radic Biol Med, 79 (2015) 14-27.

[48] Y. Luo, C.K. Chang, D. Kessel, Rapid initiation of apoptosis by photodynamic therapy, Photochem Photobiol, 63 (1996) 528-534.

[49] E. Panzarini, V. Inguscio, L. Dini, Timing the multiple cell death pathways initiated by Rose Bengal acetate photodynamic therapy, Cell Death Dis, 2 (2011) e169.

[50] N. Ahmad, S. Gupta, D.K. Feyes, H. Mukhtar, Involvement of Fas (APO-1/CD-95) during photodynamic-therapy-mediated apoptosis in human epidermoid carcinoma A431 cells, J Invest Dermatol, 115 (2000) 1041-1046.

[51] A.B. Santamaria, D.W. Davis, D.X. Nghiem, D.J. McConkey, S.E. Ullrich, M. Kapoor, G. Lozano, H.N. Ananthaswamy, p53 and Fas ligand are required for psoralen and UVA-induced apoptosis in mouse epidermal cells, Cell Death Differ, 9 (2002) 549-560.

[52] S.P. Cullen, S.J. Martin, Caspase activation pathways: some recent progress, Cell Death Differ, 16 (2009) 935-938.

[53] M. Kruidering, G.I. Evan, Caspase-8 in apoptosis: the beginning of "the end"?, IUBMB Life, 50 (2000) 85-90.